ChemComm

Accepted Manuscript

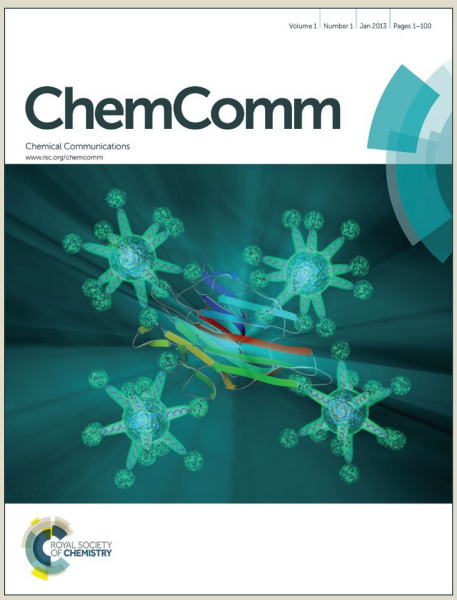

This is an *Accepted Manuscript*, which has been through the Royal Society of Chemistry peer review process and has been accepted for publication.

Accepted Manuscripts are published online shortly after acceptance, before technical editing, formatting and proof reading. Using this free service, authors can make their results available to the community, in citable form, before we publish the edited article. We will replace this *Accepted Manuscript* with the edited and formatted *Advance Article* as soon as it is available.

You can find more information about *Accepted Manuscripts* in the Information for Authors.

Please note that technical editing may introduce minor changes to the text and/or graphics, which may alter content. The journal's standard Terms & Conditions and the Ethical guidelines still apply. In no event shall the Royal Society of Chemistry be held responsible for any errors or omissions in this *Accepted Manuscript* or any consequences arising from the use of any information it contains.

ROYAL SOCIETY OF CHEMISTRY

www.rsc.org/chemcomm

Please do not adjust margins

Journal Name

COMMUNICATION

Highly-oriented $Fe_2O_3/ZnFe_2O_4$ nanocolumnar heterojunction with improved charge separation for photoelectrochemical water oxidation

Received 00th January 20xx,
Accepted 00th January 20xx

DOI: 10.1039/x0xx00000x

www.rsc.org/

Zhibin Luo,[a,b] Chengcheng Li,[a,b] Dong Zhang,[a,b] Tuo Wang*[a,b] and Jinlong Gong*[a,b]

This paper describes the design and synthesis of a heterojunction photoanode comprised of highly-oriented $Fe_2O_3/ZnFe_2O_4$ nanocolumnar arrays with well-defined morphology by reactive ballistic deposition and atomic layer deposition. This specific structure enhances the charge separation at the $Fe_2O_3/ZnFe_2O_4$ interface, leading to an improved photoelectrochemical performance for water oxidation.

Hematite (α-Fe_2O_3) is currently considered to be a promising candidate for solar hydrogen production.[1] However, poor conductivity, short hole diffusion length (2-4 nm) and sluggish oxygen evolution kinetics are intrinsic limitations of hematite for effective solar water splitting.[2] Various strategies have been proposed to address these obstacles, including element doping[3], nanoconstructuring,[4] and surface modifications.[5] Grätzel and coworkers fabricated Si-doped dendritic hematite films with an outstanding photoelectrochemical (PEC) performance.[3] Sn-doped hematite nanowires synthesized by Li and coworkers also show a remarkable photocurrent density.[6] Sivula et al. demonstrated that mesoporous hematite yields impressive water oxidation photocurrents.[7] The $Fe_2O_3/Fe_2TiO_5/TiO_2$ heterostructure reported by Zhong and Sun exhibits an extraordinary PEC performance owing to the reduced hole accumulation.[8] Wang and colleagues attained a recorded turn-on voltage of 0.45 V vs. reversible hydrogen electrode (RHE) with $NiFeO_x$ cocatalyst.[9]

Tailoring Fe_2O_3 with desired 1-D arrayed heterojunction nanostructure offers essential advantages (including a short diffusion passway for facile charge transportation and large surface area for efficient interfacial charge collection) to address the limitations of Fe_2O_3.[10-12] Zinc ferrite ($ZnFe_2O_4$) is an ideal semiconductor with a bandgap of 1.9-2.0 eV and suitable band-edge positions to form staggered type-II heterojunction relative to TiO_2, ZnO, Fe_2O_3.[13] Noticeable improved PEC photoconversion capabilities were observed with a $TiO_2/ZnFe_2O_4$ nanotube array structure and a three-dimensional $ZnO/ZnFe_2O_4$ nanorod array structure.[11,12] However, the preparation methods for these structures induced severe aggregation or pore sealing of the nanostructure, hampering their performance.

In this study, we design and fabricate a highly-oriented $Fe_2O_3/ZnFe_2O_4$ in 1-D nanocolumnar arrays to construct nanoscale heterojunctions with well-defined morphology employing reactive ballistic deposition (RBD) of Fe_2O_3 core and atomic layer deposition (ALD) of ZnO followed by air annealing that forms $ZnFe_2O_4$. This $Fe_2O_3/ZnFe_2O_4$ heterojunction can effectively facilitate the charge separation at the interface, thus leading to an enhanced PEC water oxidation performance. A brief schematic illustration of the sample preparation procedure is shown in Scheme S1 (Details in ESI). The optimized Fe_2O_3 nanocolumnar array films in our study were deposited at an incident angle of 75° respected to the substrate normal with a film thickness of approximately 200 nm. In the remainder of this paper, we denote the prepared heterojunction photoanode as $Fe_2O_3/ZnFe_2O_4$(x nm), where x indicates the thickness of $ZnFe_2O_4$ overlayer.

The formation of $ZnFe_2O_4$ in the solid state reaction of Fe_2O_3 and ZnO was confirmed by X-ray diffraction (XRD) (Fig. S1, ESI). The XRD spectra show that the diffraction peaks originating from $ZnFe_2O_4$ (JCPDS No. 79-1150, 2θ = 30.0°, 35.4°) raise in intensity with thicker $ZnFe_2O_4$ overlayers. The scanning electron microscope (SEM) images of bare Fe_2O_3 and $Fe_2O_3/ZnFe_2O_4$ exhibit similar morphology with plenary nanoporous structures (Fig. 1a, b), demonstrating that the 1-D arrayed nanostructure of the backbone Fe_2O_3 sample remains fundamentally intact upon the formation of $ZnFe_2O_4$ overlayer. The conformal formation of $ZnFe_2O_4$ stems from the conformal ALD growth of ZnO layer with controllable thickness in atomic scale,[14,15] and the fact that the morphology of the ALD-grown ZnO layer could be preserved after the solid state reaction with Fe_2O_3. This coating strategy provides a unique advantage

[a] Key Laboratory for Green Chemical Technology of Ministry of Education, School of Chemical Engineering and Technology, Tianjin University.
[b] Collaborative Innovation Center of Chemical Science and Engineering Tianjin 300072, China. E-mail: wangtuo@tju.edu.cn; jlgong@tju.edu.cn.

Electronic Supplementary Information (ESI) available: experimental details including fabrication methods, schematic illustration, XRD, UV-vis, IPCE, etc. See DOI: 10.1039/x0xx00000x

ChemComm Accepted Manuscript

Please do not adjust margins

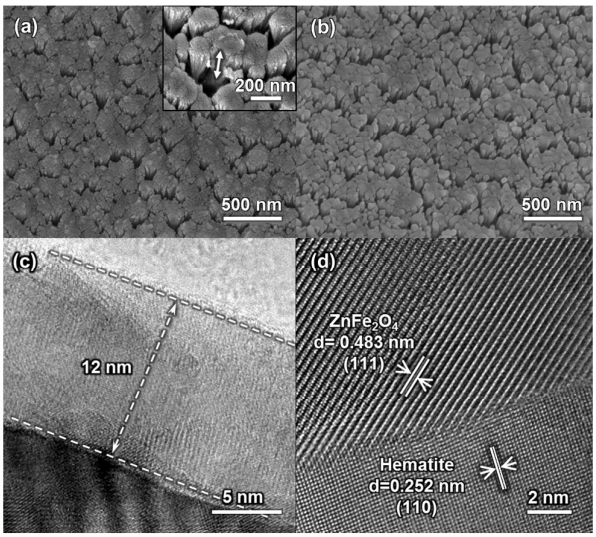

Fig. 1 SEM images of (a) Fe_2O_3 and (b) $Fe_2O_3/ZnFe_2O_4$ nanocolumnar array thin films; The inset shows a single nanocolumnar rod of about 200 nm (Details in ESI); TEM images of (c) a 12 nm $ZnFe_2O_4$ layer and (d) enlarged interface of $Fe_2O_3/ZnFe_2O_4$ heterojunction.

compared with traditional dipping method that tends to cause severe aggregation or blocking issues in the nanostructure.

The porosity and the surface area of $Fe_2O_3/ZnFe_2O_4$ will slightly decrease comparing with the bare Fe_2O_3, as the incorporation of zinc element into the Fe_2O_3 nanocolumnar arrays increases the total volume of $Fe_2O_3/ZnFe_2O_4$. According to the stoichiometric ratio of $ZnFe_2O_4$, the volume of $ZnFe_2O_4$ is about twice of that of Fe_2O_3 after the solid state reaction. With increasing amount of ZnO reacts with Fe_2O_3 in the solid state reaction, more Fe_2O_3 is converted to $ZnFe_2O_4$, decreasing the volume of nanocolumnar pores and reducing the surface area. On the other hand, the thickness of the $ZnFe_2O_4$ layer can be precisely controlled by tuning the solid state reaction time, while the remaining ZnO can be completely removed by NaOH etching. Thus a well-defined $Fe_2O_3/ZnFe_2O_4$ heterostructure could be formed. The optimized thickness of the $ZnFe_2O_4$ overlayer is about 12 nm (Fig. 1c).

The lattice distance of 0.48 nm in high resolution transmission electron microscopy (HRTEM, Fig. 1d) clearly indicates the existence of $ZnFe_2O_4$. A sharp and abrupt $Fe_2O_3/ZnFe_2O_4$ interface is also observed. The solid state reaction of Fe_2O_3 and ZnO creates an intimate contact at this interface, which is critical to facile charge transport.[16] The well-defined interface as well as the non-existence of the remaining top-most layer after the solid state reaction (*e.g.*, ZnO in this study, TiO_2 for Fe_2O_3/Fe_2TiO_5[8]) makes it easier to investigate the charge separate effect of the heterojunction.

A simplified band diagram of the $Fe_2O_3/ZnFe_2O_4$ heterojunction (Fig. 2a) can be obtained according to the estimated conduction and valence band edges of Fe_2O_3 and $ZnFe_2O_4$.[17,18] With this typical type-II heterojunction structure, the separation of photogenerated electron-hole pairs is expected to be accelerated at the $Fe_2O_3/ZnFe_2O_4$ interface.

PEC performance of bare Fe_2O_3 and $Fe_2O_3/ZnFe_2O_4$ heterojunction photoanodes was investigated by observing the

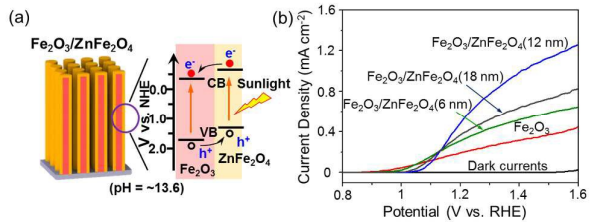

Fig. 2 (a) Theoretical conduction and valence band positions of hematite and zinc ferrite at pH 13.6.[17] (b) I-V characteristics of bare Fe_2O_3 and $Fe_2O_3/ZnFe_2O_4$ heterojunction photoanodes measured in 1 M KOH solution under AM 1.5G illumination (100 mW cm^{-2}).

current-voltage (I-V) characteristics in 1 M KOH aqueous solution under AM 1.5G illumination (100 mW cm^{-2}) (Fig. 2b). The remarkable improvement of current densities with respect to bare Fe_2O_3 clearly reveals the enhanced PEC activity upon forming $Fe_2O_3/ZnFe_2O_4$ heterojunction. An photocurrent density of 0.8 mA cm^{-2} at 1.23 V vs. RHE was achieved for the optimized $Fe_2O_3/ZnFe_2O_4$(12 nm) photoanode, which is roughly doubled compared to the value of Fe_2O_3 modified by $ZnFe_2O_4$ via aqueous solution growth method.[19] This current density is superior to all previously reported $Fe_2O_3/ZnFe_2O_4$ heterostructured anodes without cocatalyst loading.[17,19]

Fig. 2b also reveals that thicker $ZnFe_2O_4$ layer does not guarantee improved PEC performance. Excess $ZnFe_2O_4$ will induce significant pore-sealing effect (Fig. S2, ESI). Thus, thicker $ZnFe_2O_4$ leading to the loss of surface area will eventually outweigh the enhancement by the $Fe_2O_3/ZnFe_2O_4$ heterojunction.

UV-vis absorptance spectra (Fig. S3, ESI) show that the absorption edges of bare Fe_2O_3 and $Fe_2O_3/ZnFe_2O_4$ photoanode are around 600 nm, corresponding to the bandgap of Fe_2O_3; while some difference in light absorption appears at the transparent region due to interference caused by the nanocolumnar structure. Thus, light absorption would not be a crucial factor for the PEC performance, considering the relative thin thickness of $ZnFe_2O_4$. Furthermore, incident photon-to-electron conversion efficiency (IPCE) of $Fe_2O_3/ZnFe_2O_4$ photoanode exhibits significant enhancement in comparison with bare Fe_2O_3 only in the absorption region of Fe_2O_3 (Fig. S4, ESI), suggesting that the absorbed photons can be utilized more efficiently.

To rule out any possible reasons other than enhanced charge separation for the enhanced PEC performance of $Fe_2O_3/ZnFe_2O_4$ heterojunction, the following possibilities are considered. Faster surface reaction kinetics on $ZnFe_2O_4$ surface is a possible reason, while the surface passivation effect of the $ZnFe_2O_4$ layer is also a possibility.[20] To exclude these possibilities, 0.5 M H_2O_2 was added into the electrolyte as a hole scavenger (Fig. 3a,b). The dark currents of Fe_2O_3 and $Fe_2O_3/ZnFe_2O_4$ electrodes exhibit a negligible difference, indicating equally fast reaction kinetics in the presence of H_2O_2 hole scavenger, independent of Fe_2O_3 surface or $ZnFe_2O_4$ surface (Fig. 3a). Thus, any photocurrent difference between these two samples upon illumination in such an electrolyte should be due to the buried junction or the interface of the junction. Therefore, the significant photocurrent improvement of $Fe_2O_3/ZnFe_2O_4$ photoanode compared to bare Fe_2O_3 clearly

ChemComm Accepted Manuscript

This journal is © The Royal Society of Chemistry 20xx

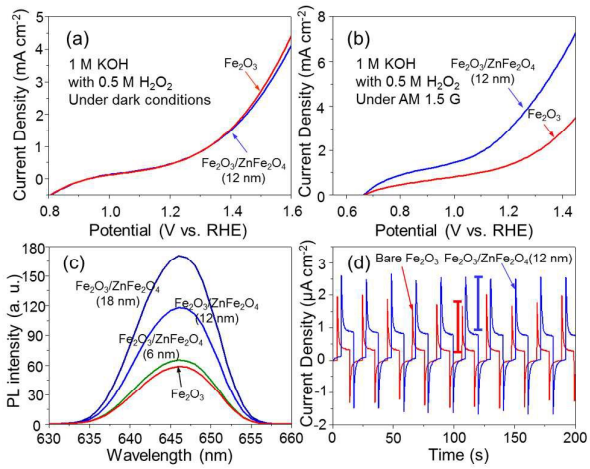

Fig. 3 I-V characteristics of Fe_2O_3 and $Fe_2O_3/ZnFe_2O_4$ heterojunction electrodes measured for H_2O_2 oxidation (0.5 M) and water oxidation under (a) darkness and (b) AM 1.5G illumination; (c) PL spectra of Fe_2O_3 and $Fe_2O_3/ZnFe_2O_4$ electrodes excited at a laser wavelength of 320 nm. (d) Transient photocurrents under chopped illumination at constant potential of 1.23 V (vs. RHE) under 420 nm illumination.

indicates an enhanced charge separation resulted from the $Fe_2O_3/ZnFe_2O_4$ heterojunction (Fig. 3b).

To further exclude the possibility that the improved PEC performance only stem from the $ZnFe_2O_4$ surface or $Fe_2O_3/ZnFe_2O_4$ interface with less surface/interface defects, photoluminescence (PL) study was performed to elucidate the effects of the $Fe_2O_3/ZnFe_2O_4$ heterojunction (Fig. 3c). The emission around 646 nm can be attributed to the recombination of photo-induced charge carriers at -OH sites or O-terminated surfaces.[21] The bare Fe_2O_3 electrode exhibits the weakest PL peak. Considering that the PL intensity reflects the rate of electron-hole recombination,[22,23] the increasing PL peak with thicker $ZnFe_2O_4$ clearly indicates that the $ZnFe_2O_4$ layer results in an unfavorable surface/interface, where more electron-hole pairs recombine as more photo-induced charge carriers transfer through the $Fe_2O_3/ZnFe_2O_4$ heterojunction owing to improved charge separation. Furthermore, transient photocurrents of the $Fe_2O_3/ZnFe_2O_4$(12 nm) photoanode at 420 nm exhibit comparable spikes to that of Fe_2O_3 upon chopped illumination (blue and red bars in Fig. 3d), illustrating serious trapping and discharging effects for charge carriers. Thus, the surface passivation of $ZnFe_2O_4$ layer is negligible. It is unlike that the improved PEC performance is caused by reduced charge accumulation at the $Fe_2O_3/ZnFe_2O_4$ interface, as reported in Fe_2TiO_5 modified Fe_2O_3.[8] Based on the PL and transient photocurrent behaviors, as well as the I-V characteristic with H_2O_2 hole scavenger, it is safe to conclude that the improved PEC performance of $Fe_2O_3/ZnFe_2O_4$ photoanode is indeed originated from the facile charge separation due to the $Fe_2O_3/ZnFe_2O_4$ heterojunction.

In conclusion, the $Fe_2O_3/ZnFe_2O_4$ photoanode prepared by highly controllable RBD and ALD techniques prevents the agglomeration or blocking issues of the nanoporous structure, leading to a well-defined $Fe_2O_3/ZnFe_2O_4$ heterojunction. A photocurrent of ~0.8 mA cm^{-2} at 1.23 V vs. RHE is obtained, which is superior to all previously reported $Fe_2O_3/ZnFe_2O_4$ heterostructured anodes. The I-V characteristics with H_2O_2 as the hole scavenger, as well as the PL and transient photocurrent study reveal that the improved PEC performance is due to the charge separation effect of the $Fe_2O_3/ZnFe_2O_4$ heterojunction. Our work demonstrates that constructing highly-oriented heterojunction with a well-organized nanostructure is an effective approach to improve the charge separation for enhanced PEC water oxidation performance. Further improvement of this $Fe_2O_3/ZnFe_2O_4$ photoanode could be attained by doping the Fe_2O_3 core to enhance charge conductivity,[6] passivating the surface states as well as loading water oxidation cocatalysts to achieve low onset potential and higher water oxidation efficiency.[20,24]

We acknowledge the National Natural Science Foundation of China (21222604, 51302185, U1463205, and 21525626), Specialized Research Fund for the Doctoral Program of Higher Education (20120032110024, 20130032120018) and the Program of Introducing Talents of Discipline to Universities (B06006), and the Natural Science Foundation of Tianjin City (13JCYBJC37000) for financial support.

References

1 S. Y. Reece, J. A. Hamel, K. Sung, T. D. Jarvi, A. J. Esswein, J. J. H. Pijpers, *Science*, 2011, **334**, 645.
2 J. H. Kennedy, K. W. Frese, *J. Electrochem. Soc.*, 1978, **125**, 709.
3 A. Kay, I. Cesar, M. Grätzel, *J. Am. Chem. Soc.*, 2006, **128**, 15714.
4 S. J. A. Moniz, J. Zhu, J. Tang, *Adv. Energy Mater.*, 2014, **4**, 1301590.
5 B. Klahr, T. Hamann, *J. Phys. Chem. C,* 2014, **118**, 10393.
6 Y. Ling, G. Wang, D. A. Wheeler, J. Z. Zhang, and Y. Li, *Nano Lett.*, 2011, **11**, 2119.
7 K. Sivula, R. Zboril, F. L. Formal, R. Robert, A. Weidenkaff, J. Tucek, J. Frydrych and M. Grätzel, *J. Am. Chem. Soc.,* 2010, **132**, 7436.
8 J. Deng, X. Lv, J. Liu, H. Zhang, K. Nie, C. Hong, J. Wang, X. Sun, J. Zhang, and S.-T. Lee, *ACS Nano*, 2015, **9**, 5348.
9 J. Jang, C. Du, Y. Ye, Y. Lin, X. Yao, J. Thorne, E. Liu, G. McMahon, J. Zhu, A. Javey, J. Guo & D. Wang. *Nat. Commun.*, 2015, **6**, 7447.
10 E. S. Kim, N. Nishimura, G. Magesh, J. Y. Kim, J. W. Jang, H. Jun, J. Kubota, K. Domen, J. S. Lee, *J. Am. Chem. Soc.*, 2013, **135**, 5375.
11 Y. Hou, X. Y. Li, Q. D. Zhao, X. Quan, G. H. Chen, *Adv. Funct. Mater.*, 2010, **20**, 2165.
12 Y. Bu, Z. Chen, W. Li, *Dalton T.*, 2013, **42**, 16272.
13 R. Marschall, *Adv. Funct. Mater.*, 2014, **24**, 2421.
14 T. Wang, Z. Luo, C. Li and J. Gong, *Chem. Soc. Rev.*, 2014, **43**, 7469.
15 C. Li, T. Wang, Z. Luo, D. Zhang and J. Gong, *Chem. Commun.*, 2015, **51**, 7290.
16 H. Yang, W. Fan, A. Vaneski, A. S. Susha, W. Y. Teoh, A. L. Rogach, *Adv. Funct. Mater.*, 2012, **22**, 2821.
17 K. J. McDonald, K. S. Choi, *Chem. Mater.*, 2011, **23**, 4863.
18 A. Kargar, Y. Jing, S. J. Kim, C. T. Riley, X. Pan, D. Wang, *ACS Nano*, 2013, **7**, 11112.
19 Y. Guo, Y. Fu, Y. Liu, S. Shen, *RSC Adv.*, 2014, **4**, 36967.
20 F. L. Formal, N. Tétreault, M. Cornuz, T. Moehl, M. Grätzel and K. Sivula, *Chem. Sci.,* 2011, **2**, 737.
21 B. Iandolo, A. Hellman, *Angew. Chem. Int. Ed.*, 2014, **53**, 13404.

ChemComm Accepted Manuscript

Please do not adjust margins

22 F. Le Formal, N. Tetreault, M. Cornuz, T. Moehl, M. Grätzel, K. Sivula, *Chem. Sci.*, 2011, **2**, 737.
23 S. Shen, J. Jiang, P. Guo, C. X. Kronawitter, S. S. Mao, L. Guo, *Nano Energy*, 2012, **1**, 732.
24 X. Chang, T. Wang, P. Zhang, J. Zhang, A. Li and J. Gong, *J. Am. Chem. Soc.*, 2015, **137**, 8356.

ChemComm Accepted Manuscript

This journal is © The Royal Society of Chemistry 20xx